Electrochemical and Surface Enhanced Raman Spectroscopic Investigation of Corrosion of Hard Disks with 1nm and 2nm Thick Overlayers of Diamond Like Carbon

Evan T. Dellor and Thomas M. Devine

Department of Materials Science and Engineering
University of California, Berkeley

Introduction

Diamond-like carbon overcoats serve to protect the magnetic media in hard disk drives against wear and corrosion. As these overcoats approach the thickness needed for the read-write head to resolve 1Tb/in^2, the corrosion mechanisms must be better understood. This understanding will aid in the development of new materials, both for the overcoat and for the magnetic media, and can be used to validate the use of fast tests for overcoat quality control. Thinner overcoats intensify the effects of through-thickness porosity and interfacial phenomena on corrosion susceptibility. We are developing electrochemical experiments that serve both as rapid corrosion susceptibility tests, and as an aid in mechanistic analysis. Additional information for this project will come from a humidity/temperature-controlled quartz crystal microbalance, as well as from surface-enhanced Raman spectroscopy.

Past investigations revealed that the rate of electrochemical reduction reactions on the surface of DLC films is fairly rapid, and that these reactions are limited by transfer of electrons through a hypothesized reaction product layer (RPL). In turn, the reduction reactions drive/limit the oxidation of the magnetic alloy exposed at pores/pinholes in the DLC. The RPL exists at the interface between the DLC and the aqueous solution. It is not known whether the RPL forms as a result of exposure to air or the aqueous solution. Thin (<10nm) films of DLC do not block electron flow. Thus, a better understanding of the structure and composition of the RPL would be an important step in limiting the severity of corrosion under thin films of DLC.

The earlier studies found that the electrochemical results were independent of DLC dopants, thickness, and mode of deposition. The present study investigates further the dependence of electrochemical results on DLC thickness and type, as well as on the presence or absence of lubricant. We utilized potentiodynamic polarization and potentiostatic electrochemical impedance experiments to further the RPL hypothesis.

Experimental

Samples were used as provided by industrial manufacturers, without any additional cleaning or preparation. All electrochemical tests (unless otherwise noted) were performed in an aerated standard borate buffer solution (0.01M boric acid, 0.01M sodium borate decahydrate, and 0.1M sodium chloride). The details of the electrochemical cell will be described in a separate report. An important aspect of this cell is worth noting

here. The only mechanical contacts to the sample are remote from the area exposed to the electrolyte. This ensures that the surface films, such as the DLC, are not stressed or damaged in the region being tested.

17 samples were tested with two primary types of electrochemical experiments. DLC of both the a-C:H and hybrid types were tested at 3,6, and 9nm of thickness, and these 6 were tested both with and without the presence of an organic lubricant. Media with 1 and 2nm of a-C:H:N, with and without lubricant, was also tested. In addition, several tests were performed on vertically oriented media.

All potentials noted here are with respect to an Ag-AgCl reference electrode. Potentiodynamic polarization tests involved polarizing the cell at 1mV/s from the free corrosion potential (~0.1V) to –1.0V, then to 1.0V, and back to 0V. For the vertical media, as well as the 1 and 2nm a-C:H:N, an additional test was performed. The upper limit of the sweeps was kept at 0.4V to avoid pitting the alloy, and the lower limits kept to –0.6V to avoid excessive hydrogen ion reduction. These sweeps were repeated 3 times. Then the lower limit was changed to –1.0V, so as to reduce hydrogen ions, and the sweeps repeated three times with the same upper limit. Then all 6 sweeps were repeated immediately.

The electrochemical impedance tests monitored the impedance of the cell as a function of frequency and applied dc bias. A 10mV r.m.s. amplitude sinusoidal voltage perturbation was used to stimulate a current response. A Solartron frequency response analyzer and potentiostat (models 1250 and 1287) applied the perturbations and output the complex impedance. The Scribner impedance software was used to record and analyze the output. Impedance was recorded at 10 logarithmically-spaced times per decade, spanning 65kHz to 1.0mHz. For the 1 and 2nm a-C:H:N media, the lower limit of the frequency sweeps was 10mHz. The dc biases, in experimental order, were 0, -0.2, -0.4, 0.2, 0.4, and 0.6V. The current was allowed to stabilize for 20 minutes prior to collecting the impedance data at each potential. Furthermore, the corrosion potential was allowed to stabilize for 3 hours prior to all electrochemical tests.

Surface Enhanced Raman Spectroscopy (SERS) is relatively new for us in application to magnetic recording media. For the data presented here, we used a He-Ne laser as incident radiation. Gold was deposited electrochemically from a solution of aerated 0.5mM gold chloride. The potential was held at –0.7V vs. an Ag-AgCl reference until 0.22C of charge passed. The samples were rinsed in deionized water and dried in nitrogen. An electrochemical cell was constructed to allow for the application of potentials in the borate buffer solution and simultaneous SERS measurements. The potential was stepped in 200mV increments from 0 to –0.4V, 0 to 0.8V, and back to 0V. Spectra were acquired at each potential.

Representative data is presented in the figures within the discussion section.

Results/Discussion

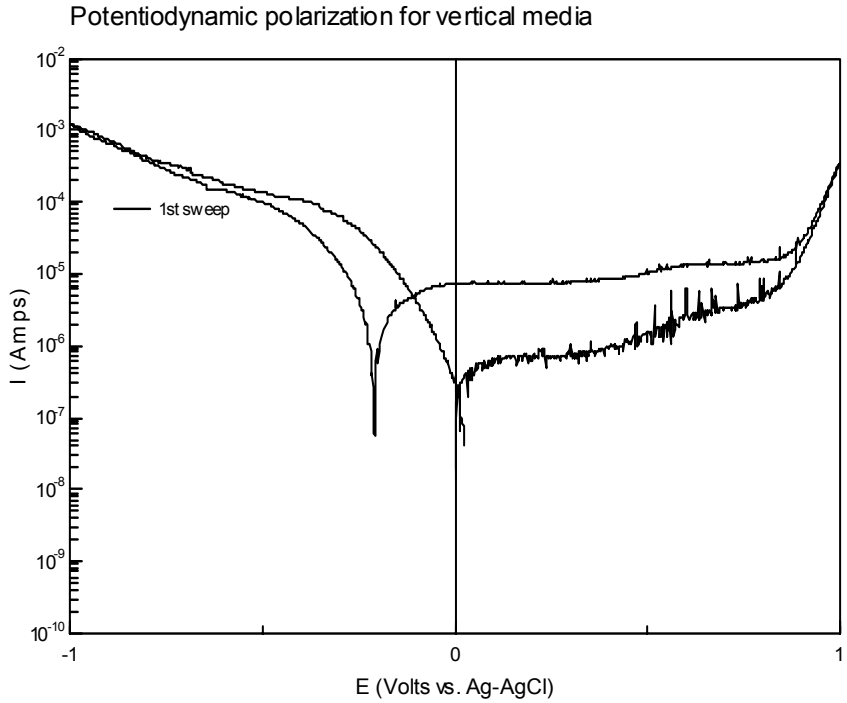

Figure 1. Polarization behavior for vertical media coated with diamond-like carbon is represented here. The sweep rate was 1.0mV/s in 0.01M $Na_2B_4O_7$, 0.01M $B(OH)_3$, plus 0.1M NaCl aqueous solution. The sweep begins at the free corrosion potential, which in this case is slightly above 0V. It then continues to –1.0V, to 1.0V, and back to 0V. This was the first sweep of 5 that were done on the same spot on the sample.

Polarization data for vertical media coated with DLC is presented in Fig. 1. During most of the sweep, the sample is not in a state it is likely to encounter in service. However, polarization to potentials far away from the free corrosion potential (E_{corr}) are needed to generate a measurable current in the external equipment. At E_{corr}, no current flows through the experimental electrochemical cell. It is reasonable to assume that at potentials near E_{corr}, the same reactions are occurring that would be if the system was exactly at E_{corr}. Thus, by polarizing away from E_{corr}, we can amplify the driving force for the reactions that occur on the surface of the sample in the same solution. Polarization to potentials farther away from those close to E_{corr} can be useful in discerning other reactions that have known potential windows. Recognizing where these reactions are occurring can help to assign an outer limit to the window most relevant for reactions that are most likely to occur in service.

Fig. 1 illustrates that the reduction current, or the current that dominates the flow at potentials below E_{corr}, is at least an order of magnitude greater than the oxidation current that flows at potentials above E_{corr}. This illustrates that passing a reduction current is easier than passing an oxidation current. The electrochemical reduction reactions, or

those that serve to pass electrons from the metal to species in the aqueous solution, must be occurring across the majority of the sample surface. This current is much too large for it to be occurring only at pores in the DLC. Previous results indicated that the transport of electrons is not limited by the DLC thickness. Experiments on bare metal, and with gold coatings over the DLC, rule out a rate limiting step of transport from the metal to the DLC, and suggest the presence of a thin (~1nm) layer that is similar for all DLC types and quantities. The rate of transport through this hypothesized reaction product layer (RPL) determines the rate of electrochemical reduction reactions, which drive the oxidation of the magnetic alloy exposed at pores.

Most of the anodic or oxidation regime illustrates that the current is independent of the potential. This type of behavior in metals is indicative of the presence of a passive film that protects metals against corrosion and thickens with potential. Other sources of oxidation could come from hydrogen that is absorbed in or adsorbed on the DLC. There are at least two sources of hydrogen that might be oxidized during anodic polarization. First is the hydrogen that is deliberately added to the carbon during the synthesis of the DLC. Second is hydrogen that is generated by the electrochemical reduction of water during the cathodic polarization of the disk. The electrochemical history of the sample is relevant. For the experiment represented by Fig. 1, the sample was first polarized to –1.0V, where a significant amount of hydrogen gas is expected to be evolved as a consequence of the reduction of hydrogen ions in solution. Oxidation of this residual hydrogen could contribute to the oxidation current that is passed during the anodic portion of the sweep. At potentials close to 1.0V, water can be expected to break down with the accompanying evolution of oxygen. This is most likely the cause of the sudden increase in current near 1.0V in Fig. 1.

It is important to note that the state of the system during a potentiodynamic polarization sweep is far from steady-state, and parameters such as E_{corr} have their meanings obscured. The apparent shift in the potential where current is 0 is a result of the system requiring a finite amount of time to reach steady state.

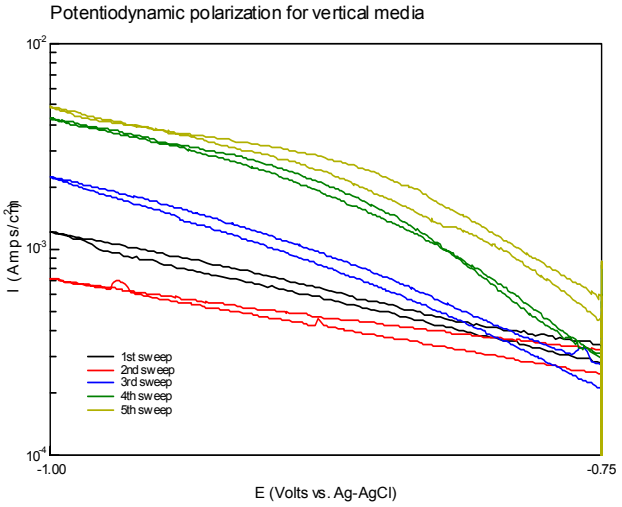

Figure 2. This plot shows a zoom of the region near -1.0V for the data in Fig. 1, and for four more sweeps that were carried out sequentially on the same sample area. In general, sequential sweeps passed more current.

Fig. 2 illustrated the increase in current that accompanies repetition of the potential sweep. The sample is clearly able to pass a reduction current more easily as a result of its electrochemical history, which in this case was the polarization up to and back from 1.0V. More hydrogen is present either as a result of this history, the surface has a lower energy barrier for the reduction of hydrogen, or the RPL has changed in nature. Current values span an order of magnitude at –1.0V. Polarization to potentials above 0.5V will severely delaminate/pit the DLC and metals underneath, as long as they are held at those potentials for some length of time. This was illustrated in past studies that found a sudden and erratic change in low frequency impedance parameters at potentials between 0.6 and 0.8V. This same behavior was not noted for the potentiodynamic sweeps, which are short in comparison to the length of time the samples spend at high potentials for the impedance tests. Both time and potential determine the catastrophic breakdown of the metal under the DLC, which is not necessarily an indicator of the corrosion susceptibility of the samples in service. They are unlikely to experience such oxidizing potentials. The time and potential characteristics of this breakdown could be an indicator of the porosity of the DLC, which indirectly influences the corrosion susceptibility. In order to avoid the complications associated with these higher potential regimes, further cyclic tests were performed at potentials below 0.4V.

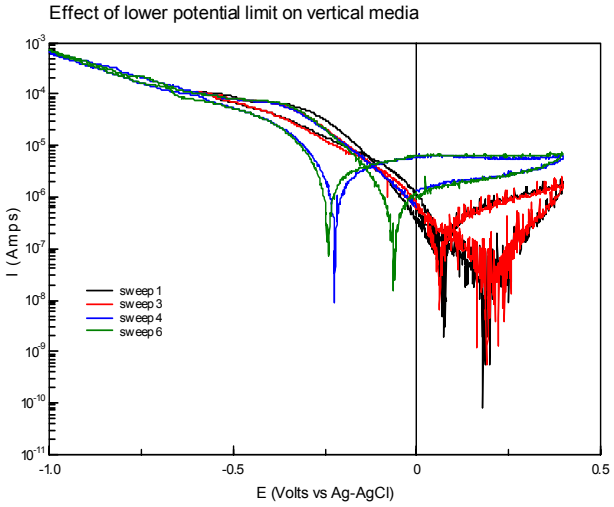

Figure 3. Potential in the experiment represented by this figure was limited to –0.6V for three sequential sweeps, with an upper limit of 0.4V. Three sequential sweeps were then limited to –1.0V. The upper limit for all sweeps was 0.4V. The 1st, 3rd, 4th, and 6th sweeps are plotted here. The sample was vertical media coated with 2.5nm DLC.

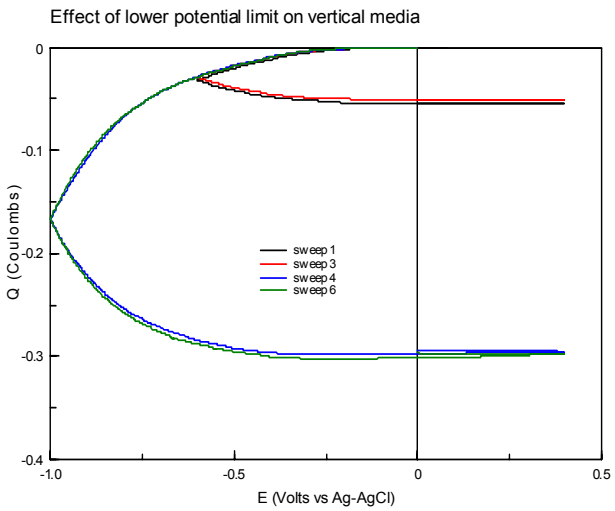

Figure 4. Plotted here is the same data as in Fig. 3, with the units converted from amps to coulombs. The charge was reset to 0 after each sweep, so that all sweeps would begin from the same value of charge.

Figure 3 illustrates the effect of limiting the lower potential of the sweeps on vertical media. Repetition of the sweeps with the same potential limit were performed to ascertain the reversibility of the reactions that occur throughout the entire regime. This figure clearly shows that the reactions are reversible, which means that they do not involve pitting of the metal or delamination of the DLC. In turn, this offers support to the validity of the impedance measurements, which require the current responses to the potential perturbation to be reversible. Notable in this figure is the large increase in the oxidation current that accompanies the lowering of the lower potential limit to –1.0V The window from –0.6 to –1.0V is diffusion limited in regards to the reduction of dissolved oxygen, and appreciable hydrogen evolution is expected to occur. If this hydrogen remains in close proximity to the DLC, either from absorption or adsorption, then it would be expected to find an increase in the sequential oxidation current due to oxidation of this residual hydrogen. This plot supports such a hypothesis.

Figure 4 demonstrates that about 5x more charge is transferred for the sweeps that continue to the regime where hydrogen ions are appreciably reduced. Furthermore, the oxidation rates pale in comparison to the amount of charge transferred during the reduction current region. Together, these plots indicate that the presence of hydrogen in the DLC films could have chemical, rather than just electrical ramifications on the corrosion limiting capabilities of the films.

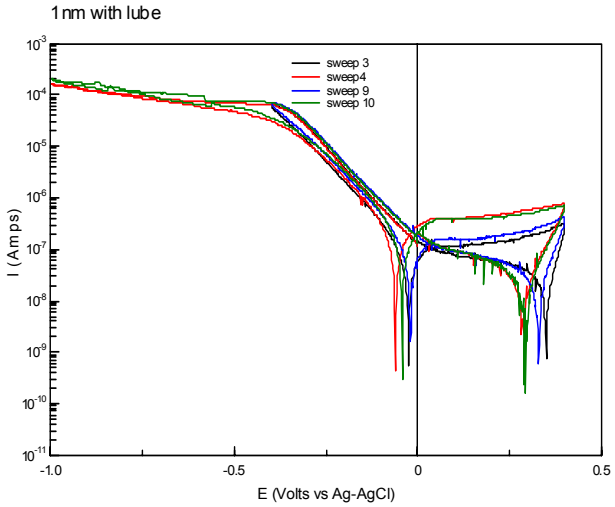

Figure 5. Potential in the experiment represented by this figure was limited to –0.4V for three sequential sweeps, with an upper limit of 0.4V. Three sequential sweeps were then limited to –1.0V. All six of these were then repeated. The upper limit for all sweeps was 0.4V. The 3rd, 4th, 9th and 10th sweeps are plotted here.

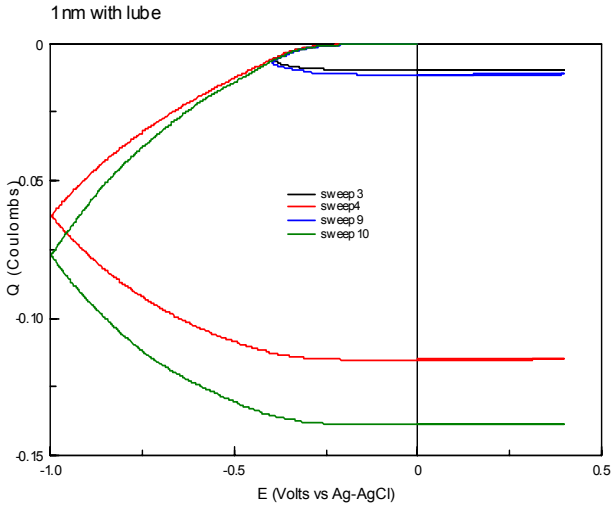

Figure 6. Plotted here is the same data as in Fig. 5, with the units converted from amps to coulombs. The charge was reset to 0 after each sweep, so that all sweeps would begin from the same value of charge.

Figures 5 and 6, when compared to Fig. 3 and 4, clearly show quantitatively differing behaviors between the vertical media and a sample coated with 1nm DLC and a lubricant. Each plot show the effect of the lowering of the potential limit to –1.0V, and the ability of the system to return (or not) to its electrochemical behavior after the lower potential limit was restored to –0.4V. It should be noted that the lower limit for the curtailed

sweeps here was –0.4V, as opposed to the –0.6V for the vertical media. The charge vs. potential plots (Fig. 4 and 6) indicate the total amount of charge involved while the system is in the reduction dominated potential range (i.e., below 0V). Because the oxidation current densities are significantly less than the reduction current densities, the amount of charge involved in oxidation currents is not clearly discernable in these plots. Oxidation behavior is more evident through inspection of the positive potential range in the log current vs. potential figures.

Nominally 3x the charge was passed for the vertical media when compared to the lubed 1nm coating. This is most likely due to the presence of the lubricant as opposed to the DLC type and thickness, as we have consistently noted the protective capabilities of the lubricant. The six additional sweeps were carried out to probe the ability of the system to return to its initial state, as in when the lower potential limits were kept to –0.6V. Of qualitative difference between the two samples is the increase in the magnitude of charge passed for the 1nm coating, as a result of more potential sweeps and longer exposure to the aqueous solution. Debonding of the lubricant from the DLC might be occurring to some degree, and this could explain the observed behavior.

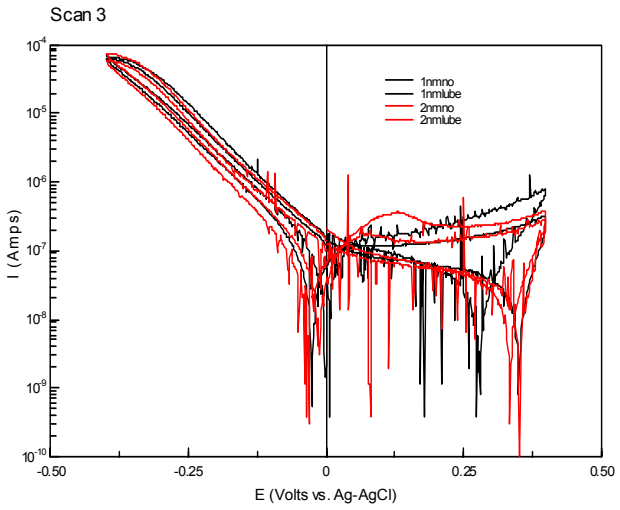

Figure 7. Representative data from experiments identical to the previous 4 figures is shown here. The plots compare the electrochemical hysteretic behavior of four samples. DLC coatings of 1 and 2nm, with and without lubricant, differentiate the data sets. The lower limit here is –0.4V.

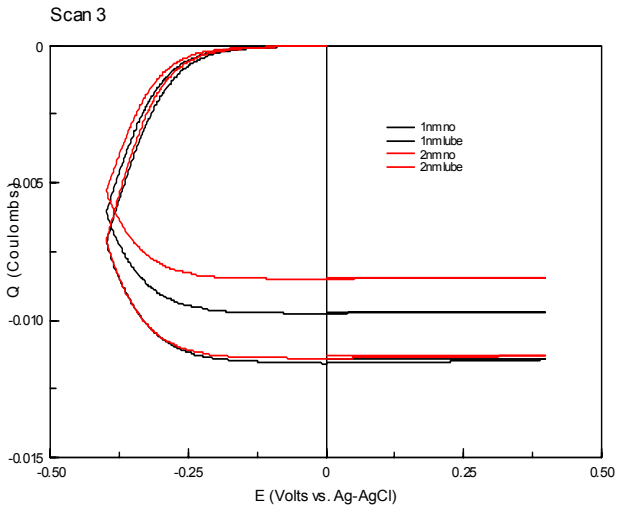

Figure 8. The same data as in Fig. 7, with the units converted to coulombs.

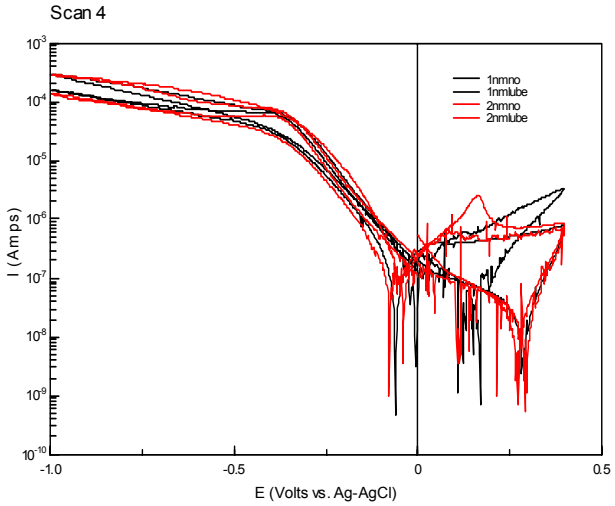

Figure 9. The plots compare the electrochemical hysteretic behavior of four samples. DLC coatings of 1 and 2nm, with and without lubricant, differentiate the data sets. The lower limit here is –1.0V. Three sweeps limited to –0.4V occurred previously to the sweeps shown here, for all samples.

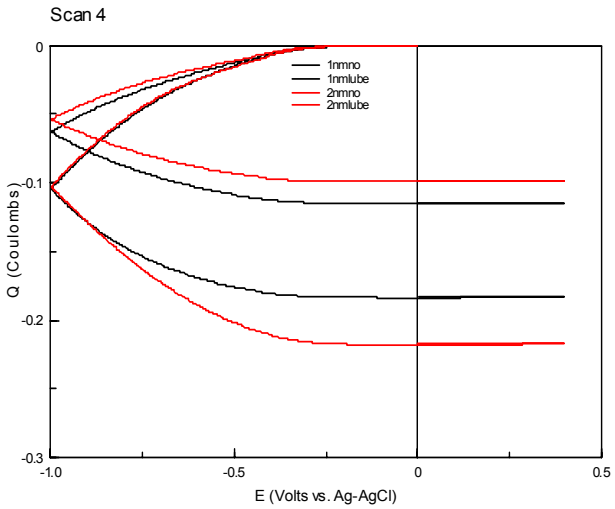

Figure 10. The same data as in Fig. 9, with the units converted to coulombs.

Figures 7-10 compare the performance of samples with 1 and 2nm DLC, with and without lubricant. Scans with both –0.4 and –1.0V as lower potential limits are represented. When the lower potential limit was –1.0V, nominally double the reduction charge was passed for the unlubed samples when compared to the lubed samples (Fig. 9 and 10). Less stark was the difference when the system was not allowed to enter the hydrogen ion reduction regime (Fig. 7 and 8, more clearly in fig. 8). In terms of resistance to passage of reduction current above –0.4V, the samples without lubricant behaved identically.

The trends are tabulated in the following two figures.

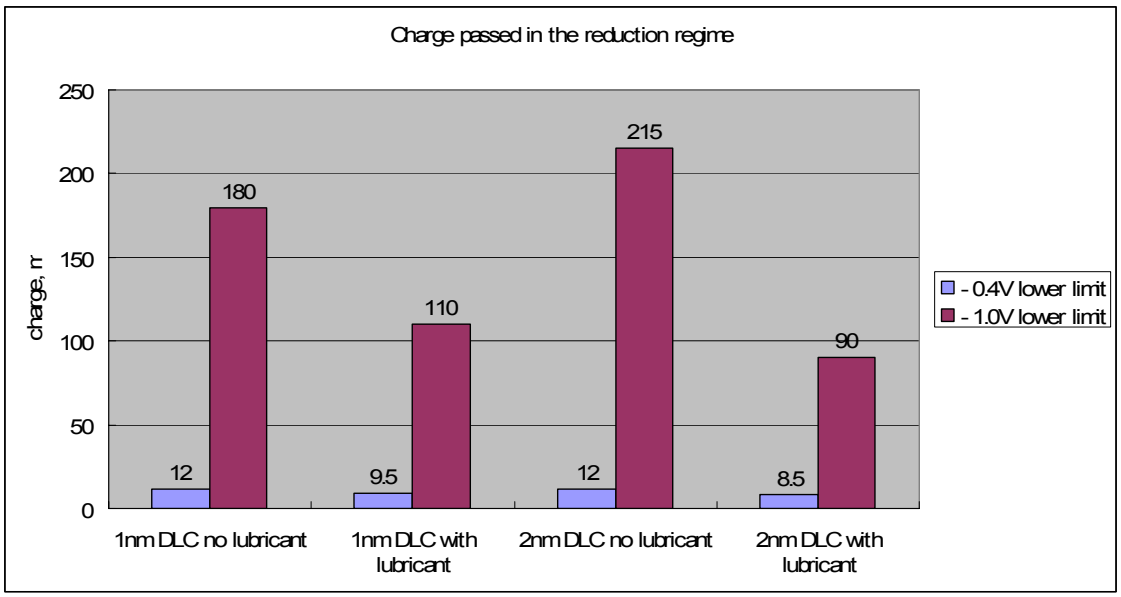

Figure 11. Charge passed in the reduction regime, with units in mC. This chart compares the effect of DLC thickness, the presence of the lubricant, and the lower potential limit in the reduction regime.

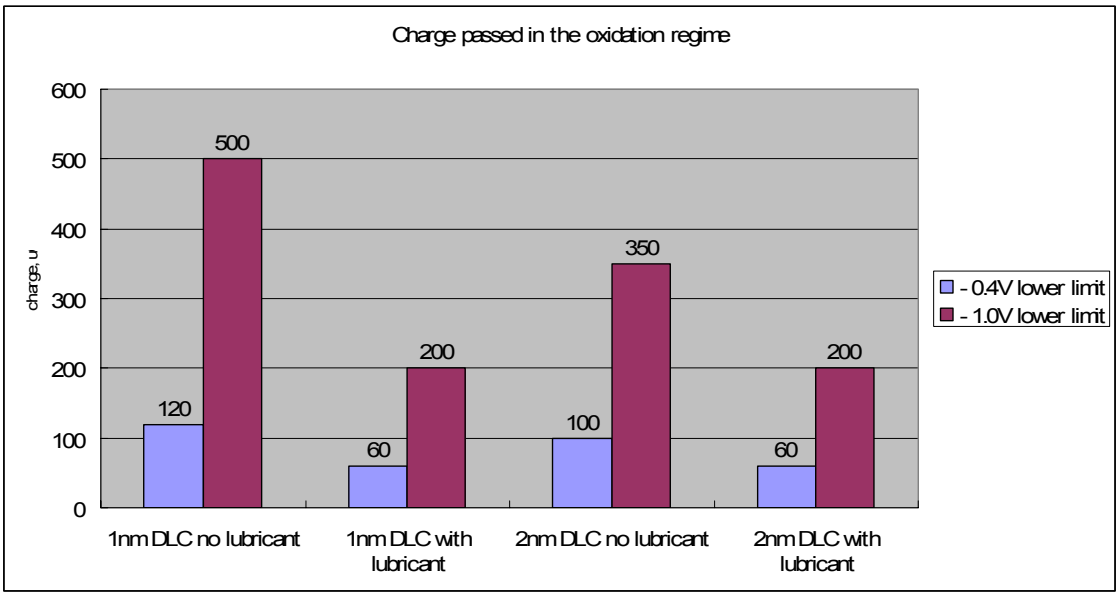

Figure 12. Charge passed in the oxidation regime, with units in μC. This chart compares the effect of DLC thickness, the presence of the lubricant, and the lower potential limit in the reduction regime.

The most notable trend is that the lubricant decreased the amount of charge passed in both regimes, for both lower potential limits, and for both quantities of DLC. Because this data is from the third and fourth polarization sweeps, the samples had already experienced the entire ranges of potential from –1.0 to 0.4V. Because the presence of the lubricant generated measurable differences in the data values, it must still be bonded to the DLC. In Fig. 12, the difference between the two values for each sample represents the additional oxidation charge passed due to the extension of the lower potential limit, i.e., from –0.4 to –1.0V. It would involve roughly 1mC of charge to oxidize hydrogen if it occupied every surface site on the DLC. Other sources of hydrogen would be that absorbed into the DLC, either from the deposition process or as a result of the extensive hydrogen ion reduction in the extended reduction regime, and from residual hydrogen in the solution. The most likely source is surface adsorbed and absorbed hydrogen, not dissolved hydrogen. If the oxidation process was utilizing dissolved hydrogen, this might severely compromise the service performance of the disks, as hydrogen is often specifically engineered into the DLC for tribological reasons. Because the difference in oxidation charge was less than 1mC, utilization of adsorbed hydrogen cannot be ruled out as a possibility. Thicker films tended to have less of a difference, which might suggest a mechanism contrary to this hypothesis. However, the hydrogen content of these DLC films is unknown to us. It does seem to indicate that hydrogen is not absorbing into the

DLC due to electrochemical reduction of hydrogen ions in the solution. These total charge quantities do not only involve hydrogen. Reduction of dissolved oxygen, for example, is a competing reduction reaction, and would be the dominant reaction at potentials less than, but close to the free corrosion potential.

.

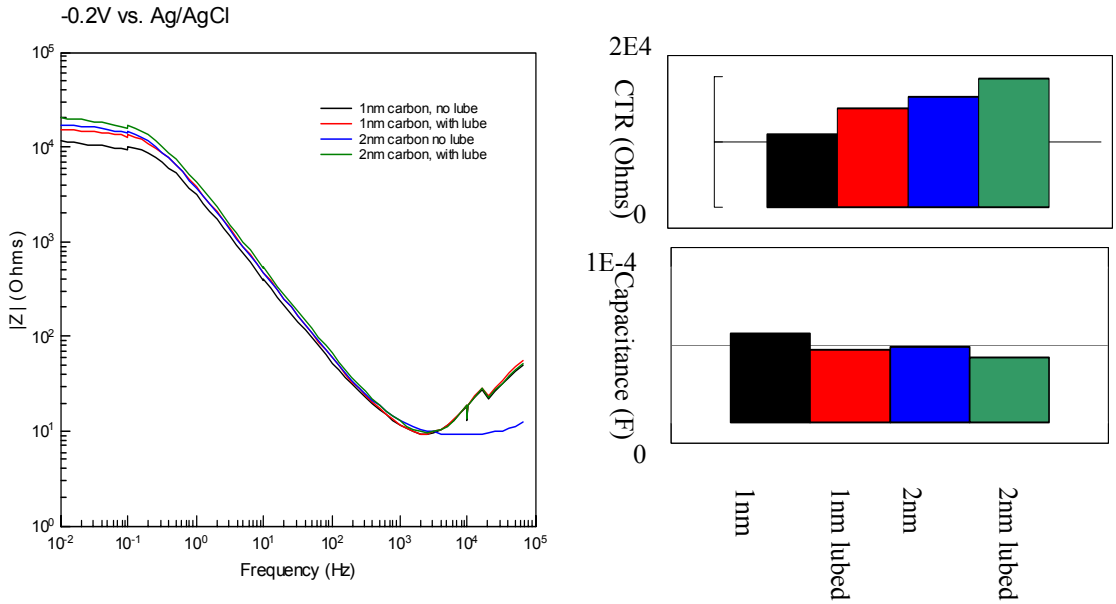

Figure 13. Cathodic impedance data for 4 samples at –0.2V. Capacitance and charge transfer resistance (CTR) values were determined from an equivalent circuit fit.

Impedance data can probe several electrochemical parameters of the system while it remains at a dynamic equilibrium. Such a state exists at a constant potential, after the current has stabilized to a constant value. The small potential oscillation used to probe the system does not alter it irreversibly. Figure 13 depicts the impedance spectra of four samples at –0.2V, as well as some of the extracted parameters. When the frequency is very low, capacitive effects can be ignored, and the resistive charge transfer behavior extracted. The value of the charge transfer resistance (CTR) is a measure of the combined resistance of the system to all electrochemical reactions that are active at the indicated potential. In this case, the predominant reaction is likely the reduction of dissolved oxygen. Resistance to reduction reactions is relevant to corrosion reactions because they always accompany those oxidation reactions. Metal available for oxidation is present only at a small percentage of the surface of DLC coated magnetic recording media. Reduction reactions can take place over the entire surface. Limiting the rate at which electrons become available for reduction reactions can reduce the rate of oxidation that occurs at pores/pinholes in the DLC. Comparison of the CTR at negative potentials, between various samples, can accomplish two tasks. First, it can quantify a general susceptibility to free corrosion in the same solution. Furthermore, the comparison can help support/refute mechanistic hypotheses. Impedance spectra, and the parameters

extracted from it, cannot generate mechanistic understanding independently, but suggested mechanisms must not be inconsistent with the impedance data.

For the data presented here, both the presence of the lubricant and the thicker DLC seemed to lower the rate of reduction reactions that likely accompany metal oxidation. This result is somewhat at odds with previous work, which indicated that the DLC was relatively transparent to electron flow, and that film thickness did not alter the electrochemical behavior of the samples in borate buffer solution. However, films as thin as 1nm were not included in that previous conclusion. Through-thickness porosity and surface structure become important considerations with films this thin. We are just beginning to utilize the SERS data to further our understanding of the electrochemical behavior of the DLC coated media. Some of the data is presented below.

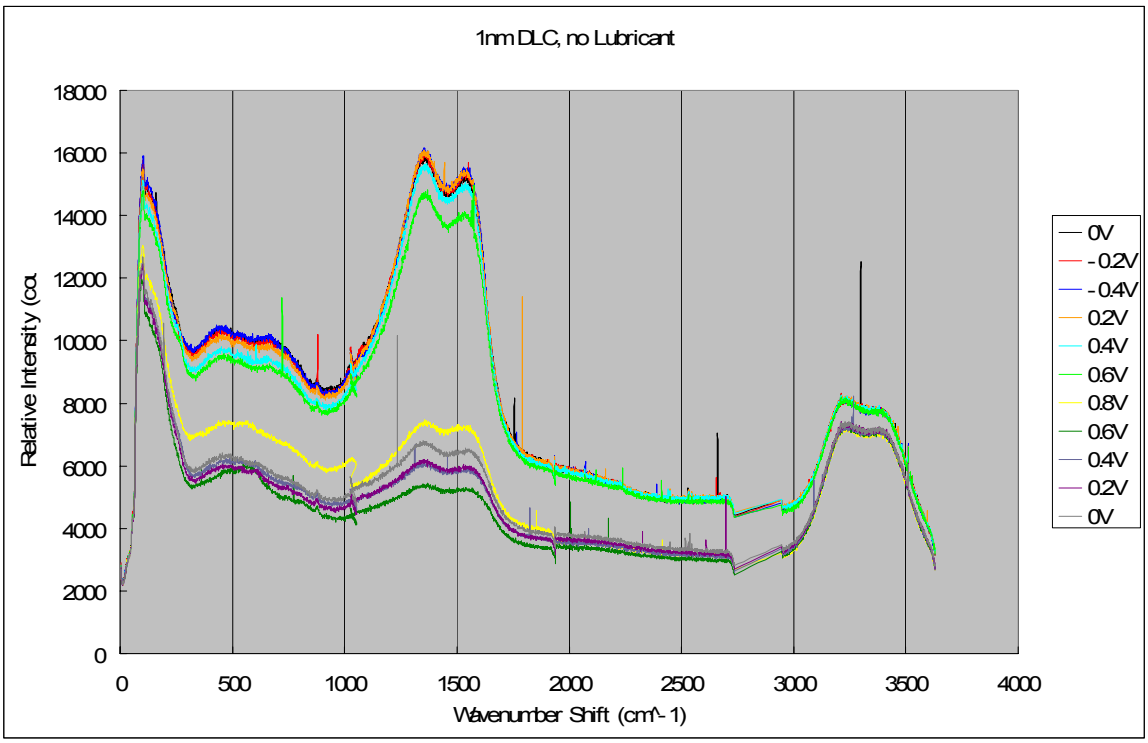

Figure 14. SERS spectra at various potentials in aerated borate buffer solution (pH 8.4). The spectra were not shifted for clarity, but left as generated to demonstrate the shifts in overall intensity as a function of potential. This sample had 1nm DLC without lubricant.

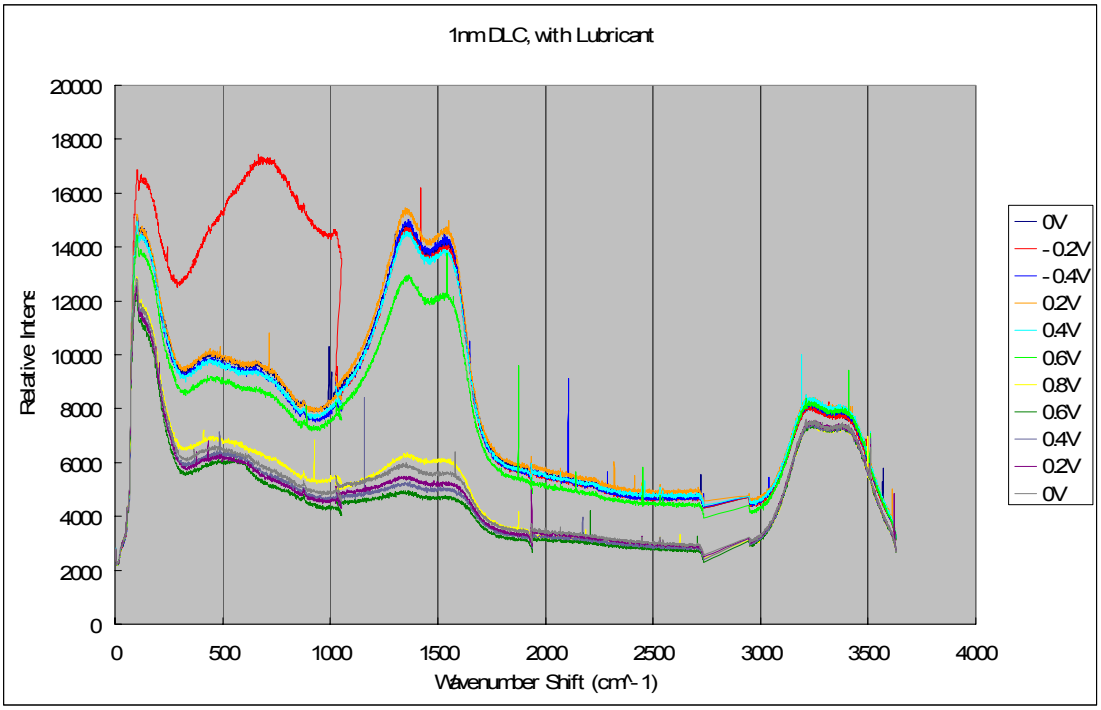

Figure 15. SERS for 1nm DLC, with lubricant.

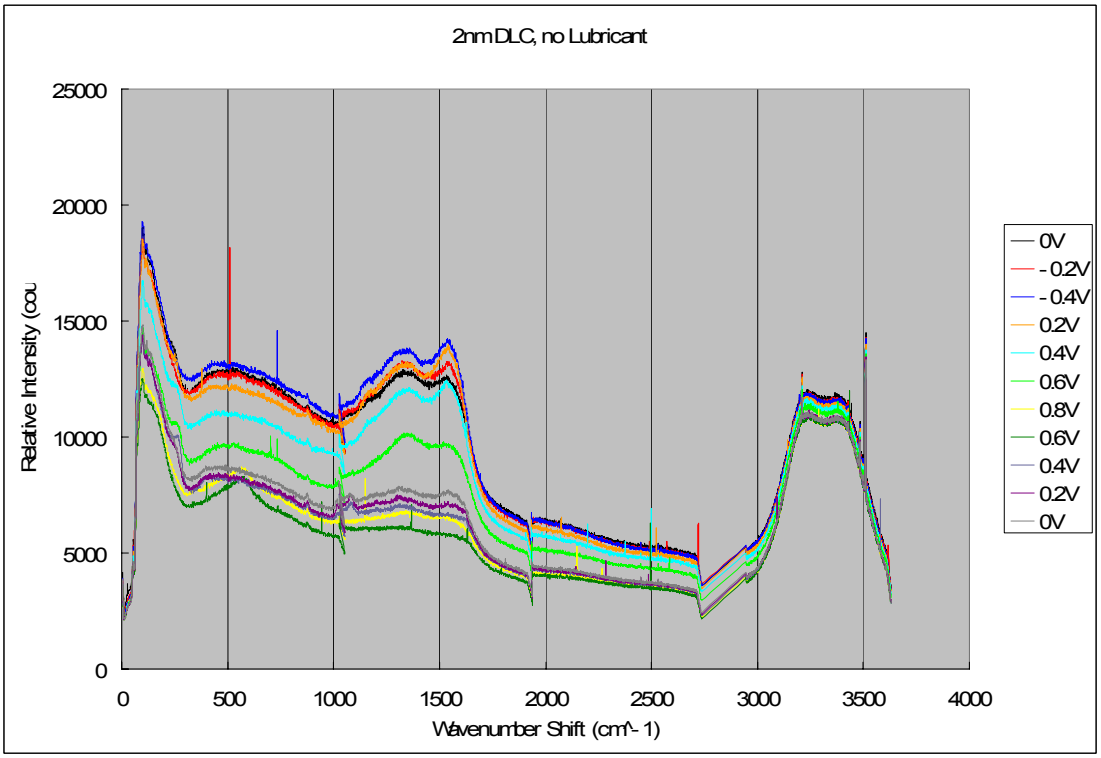

Figure 16. SERS for 2nm DLC, without lubricant.

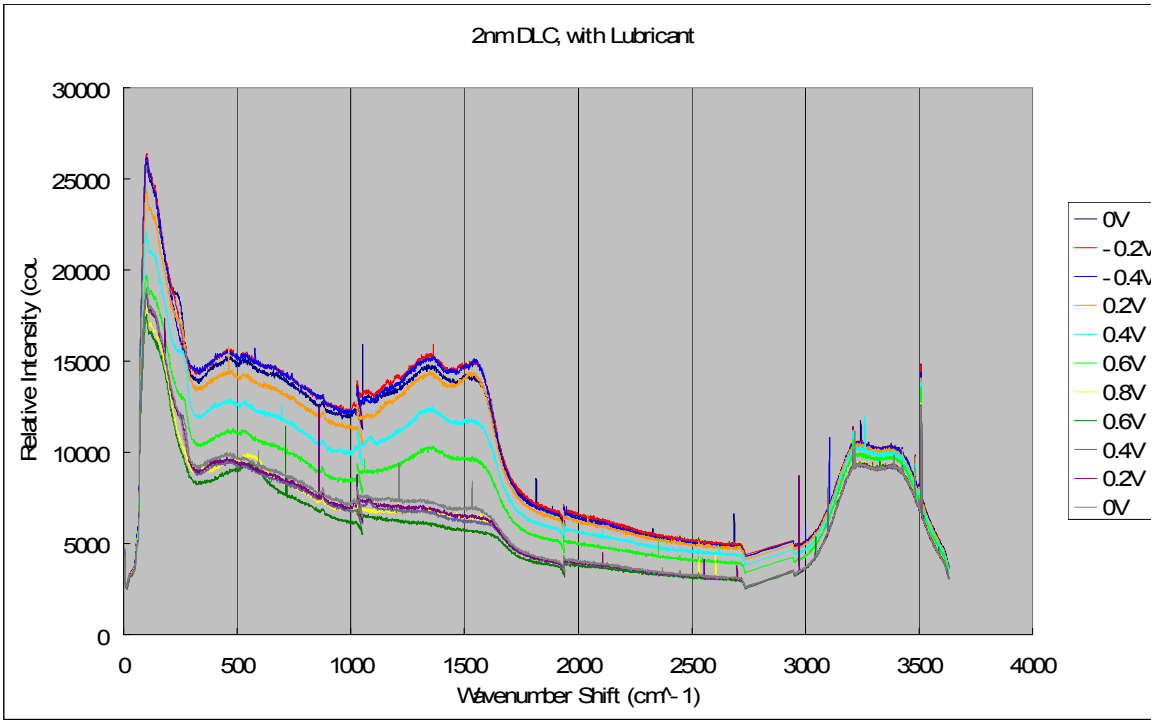

Figure 17. SERS for 2nm DLC, with lubricant.

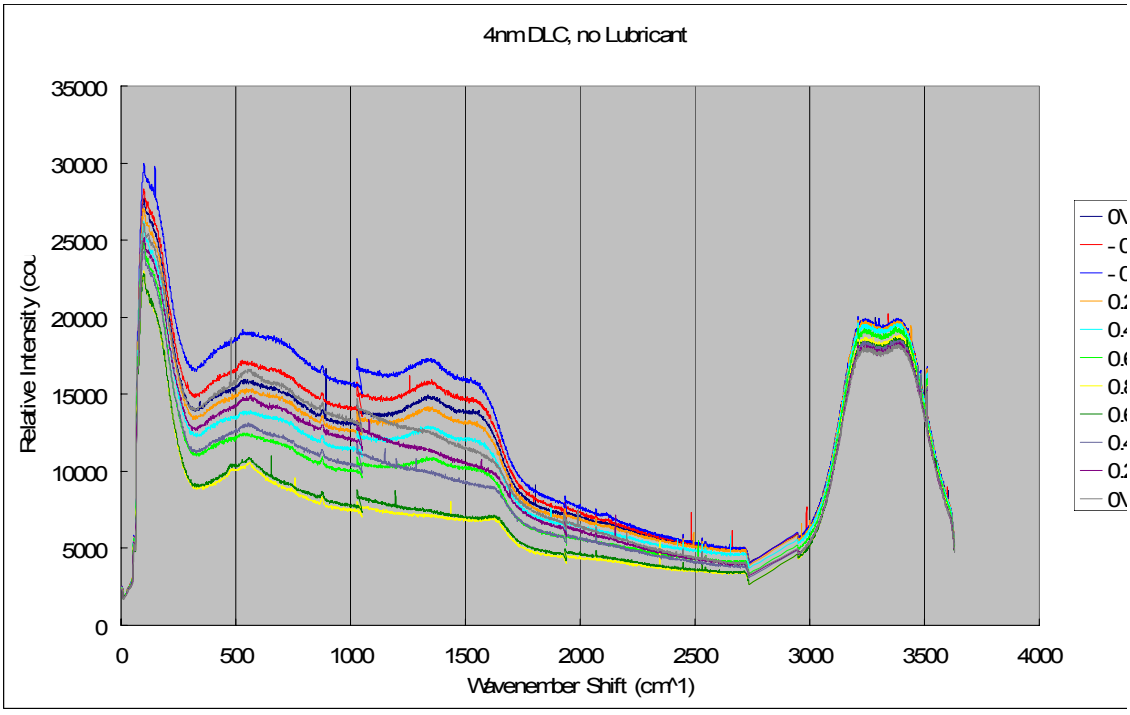

Figure 18. SERS for 4nm DLC, without lubricant.

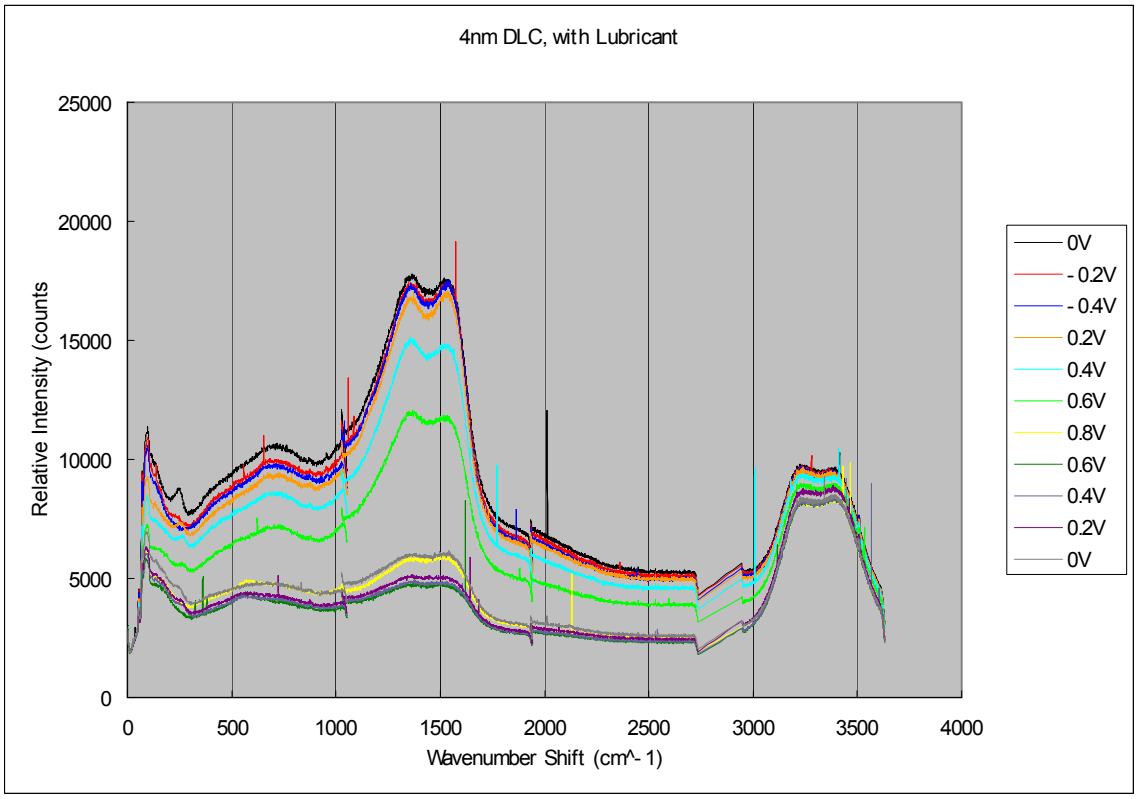

Figure 19. SERS for 4nm DLC, with lubricant.

While we have not yet analyzed all of the subtle differences between these spectra, they are consistent with out other experiments. Notably, the carbon peaks (the large double peak in the center) begin to change appreciably at potentials above 0.4V, but are relatively unchanged at potentials below 0.4V. While some of the intensity change is due to a change in the gold surface, which affects the surface enhancement, the shape of these peaks and their intensity relative to others changes with potential above 0.4V.

We are satisfied with these preliminary experiments because of the large carbon intensity, even with 1nm of DLC. In the future, we hope to identify the lubricant and more precisely identify the other dominant peaks.

Conclusions

The data demonstrate that we can quantitatively differentiate the electrochemical behavior between the sample variables. Carbon thickness seems to play less of a role in governing electrochemical behavior than does the lubricant. This is an important find, because thinner DLC films will be needed in order for recording density goals to be met. It can be assumed that the 1nm DLC films contain significant through-thickness porosity, and thus that these samples are likely to fail industrial reliability tests. Because the electrochemical behavior of these samples was not significantly different that that of the others, it seems that corrosion mitigation for samples with the thinnest of DLC films is not far off. Of specific interest here is the role of the lubricant in the electrochemical reactions that occur on the surface of the DLC.

Future Work

We will continue with a similar protocol for testing further batches of recording media. Included in these tests will be both the potentiodynamic polarization sweeps and the impedance spectroscopy scans. Films thinner than 1nm will be compared with those larger than 4nm, in order to note the sudden changes in electrochemical behavior that occurs with the thinnest films. We will also gather the SERS spectra for these samples.

Furthermore, we are working to implement a monolayer mass-measurement system utilizing a quartz crystal microbalance. We are able to independently alter the dewpoint and temperature of the sample chamber in this apparatus. These results will aid in understanding mass change due to water adsorption and oxidation of the magnetic alloy.

Acknowledgements

We are grateful to have received support from the Information Storage Industry Consortium (INSIC) and the Berkeley Computer Mechanics Laboratory, and to Seagate and DSI for providing samples. Thanks to Raj Thangaraj and Jing Gui of Seagate for offering to provide recording media and samples for the mass measurements.